PHOTONICS Research

Experimental investigation of the uncertainty principle for radial degrees of freedom

Zhihe Zhang,[1] Dongkai Zhang,[1] Xiaodong Qiu,[1] Yuanyuan Chen,[1,3] Sonja Franke-Arnold,[2,4] and Lixiang Chen[1,5]

[1]Department of Physics and Collaborative Innovation Center for Optoelectronic Semiconductors and Efficient Devices, Xiamen University, Xiamen 361005, China
[2]School of Physics and Astronomy, SUPA, University of Glasgow, Glasgow G12 8QQ, UK
[3]e-mail: chenyy@xmu.edu.cn
[4]e-mail: Sonja.Franke-Arnold@glasgow.ac.uk
[5]e-mail: chenlx@xmu.edu.cn

Received 20 September 2021; revised 30 April 2022; accepted 24 July 2022; posted 26 July 2022 (Doc. ID 443691); published 1 September 2022

While the uncertainty principle for linear position and linear momentum, and more recently for angular position and angular momentum, is well established, its radial equivalent has so far eluded researchers. Here we exploit the logarithmic radial position, $\ln r$, and hyperbolic momentum, P_H, to formulate a rigorous uncertainty principle for the radial degree of freedom of transverse light modes. We show that the product of their uncertainties is bounded by Planck's constant, $\Delta \ln r \cdot \Delta P_H \geq \hbar/2$, and identify a set of radial intelligent states that satisfy the equality. We illustrate the radial uncertainty principle for a variety of intelligent states, by preparing transverse light modes with suitable radial profiles. We use eigenmode projection to measure the corresponding hyperbolic momenta, confirming the minimum uncertainty bound. Optical systems are most naturally described in terms of cylindrical coordinates, and our radial uncertainty relation provides the missing piece in characterizing optical quantum measurements, providing a new platform for the fundamental tests and applications of quantum optics.

https://doi.org/10.1364/PRJ.443691

1. INTRODUCTION

The fact that conjugate pairs of observables cannot be simultaneously known is a central concept of quantum mechanics and quantum technologies [1–3]. It is a most concise yet quantitative statement that imposes strict constraints on the simultaneous prediction of complementary variables such as position and momentum, expressed as the familiar inequality $\Delta x \cdot \Delta p \geq \hbar/2$, which limits the product of the corresponding uncertainties by Planck's constant. Applied to the realm of optics, it has its equivalent in a Fourier relation between the profile of a light field in terms of transverse positions (x, y), and the diffraction pattern in terms of spatial frequencies (k_x, k_y), with immediate applications for the design of optical systems. Optical systems are, however, more readily described in terms of polar coordinates (r, ϕ), matching the shape of optical elements, apertures, and the Gaussian laser beam profile itself. It is therefore natural to investigate Fourier relations and associated uncertainty principles in terms of polar coordinates. Over the last decades, this has been done very successfully for the angular coordinate, and its conjugate variable, the orbital angular momentum (OAM). Early on it has been shown that these are linked by an angular uncertainty relation [4], and the OAM has been studied in the context of fundamental quantum mechanics [5–8] and for applications in communication, high-dimensional quantum protocols, and sensing [9–12], to name but a few. Since the uncertainty principle is general for any wave theory rather than a result particular to quantum mechanics, the uncertainty relation is valid for any square integrable function and its Fourier transform [13].

A complete (quantum) description of transverse light fields, however, requires us to consider not only the angular but also the radial degree of freedom [14]—yet the latter has largely been ignored. The reason for this lies in the fact that the quantum description of the radial degree of freedom and its physical interpretation is less obvious [15–17], and the generation of efficient radial modes is experimentally difficult [18]. Quantum correlations have been explored in early experiments via Hong–Ou–Mandel interference [19] and the violation of Bell inequalities [20], relating the radial index of Laguerre–Gauss modes to radial position. However, the discrete radial index cannot be mathematically derived from a continuous radial position [21,22].

According to Dirac, $\hat{p}_r$ is the "true momentum conjugate to r," which satisfies the fundamental commutation relation as $[\hat{r}, \hat{p}_r] = i\hbar$ [23], suggesting a continuous radial momentum

of the form $\hat{p}_r = -i\hbar(\partial/\partial r + 1/2r)$. This continuous radial momentum and semi-infinite radial position have been used in the experimental exploration of the Einstein–Podolsky–Rosen paradox in spatial-mode entanglement generated from spontaneous parametric downconversion [24] and radial diffraction [25]. However, the historic arguments concerning both the rigorous mathematical and physical definition of radial position and radial momentum variables still persist, leading to questions of utmost importance. First, in the semi-infinite domain of radial position, is the Dirac form of the radial momentum self-adjoint and can it present a physical observable? Second, while linear and angular position and momentum can be linked by Fourier transforms and series, what is the connection between radial position and radial momentum? Third, how to translate the mathematically defined radial operators into experimental observables?

From the perspective of practical applications, the radial degree of freedom, in combination with the angular degree of freedom, provides a new platform for high-dimensional quantum information protocols that utilize the full mode space capacity. Experimental realizations of high-dimensional entanglement in the transverse position-momentum degree of freedom are now possible with record-quality measurement speed and entanglement dimensionality [26,27], based on pixel entanglement, but not yet on modes described in rotationally symmetric coordinates. In addition, the radial degree of freedom provides a resource for quantum metrology of propagation distance or dilation, e.g., by measuring the overlap between adjoint radial modes [17], and more generally in high-resolution imaging [28].

The investigation of the radial degree of freedom has long been hailed as a requisite for the foundational understanding of quantum mechanism, but also for a variety of applications in optical communication, quantum protocols, and high-precision measurement. While Twamley and Milburn have presented elaborate theories proving that the hyperbolic momentum and logarithmic radial position can fulfill the fundamental requirement of self-adjointness [29,30], neither a complete theoretical study, nor the experimental realization of the uncertainty principle for the radial degree of freedom of transverse light modes has been explored so far.

In this paper, we exploit the logarithmic radial position and hyperbolic momentum to formulate a rigorous uncertainty principle for the radial degree of freedom. When exploring uncertainty relations, it is instructive to identify the specific states that satisfy the uncertainty, the intelligent states, which in the case of a constant bound, as we have in our case, are identical to the minimum uncertainty states. We identify the radial minimum uncertainty states and verify their uncertainty product experimentally by measuring their hyperbolic momentum spectrum. We note that the radial uncertainty relation and the identified intelligent states hold for the wave function of an individual photon. For convenience, and to decrease detrimental effects due to Poissonian noise, we confirm the shape of the radial intelligent states in the classical regime.

2. THEORETICAL FRAMEWORK

We start by defining suitable observables to describe the radial degree of freedom. According to the Dirac-von Neumann interpretation of quantum mechanics, an operator relating to an observable has to be self-adjoint, but special care has to be taken for unbounded operators on infinite or semi-infinite dimensional spaces, as is the case for the radial coordinate. As a consequence, the Dirac form of the radial momentum, $\hat{p}_r$, is not self-adjoint and hence does not relate to an observable [21,31–33], posing subtle difficulties on defining a radial uncertainty relation.

We follow earlier research in defining the hyperbolic momentum operator in the circular-cylindrical coordinate system [17,29,30] as

$$\hat{P}_H = \frac{1}{2}(r\hat{p}_r + \hat{p}_r r) = -i\hbar\left(r\frac{\partial}{\partial r} + 1\right), \tag{1}$$

where the hyperbolic momentum operator has the dimension of $\hbar$ as a direct result of its definition. While linear momentum is associated with invariance under translation, hyperbolic momentum is associated with invariance under scale translation. Therefore, the hyperbolic momentum operator generates dilation, and cannot cause the radial coordinate to be negative. We note that the domain of $\hat{P}_H$ is defined as $\psi \in \mathcal{L}^2([0, +\infty)), \psi \equiv U/r, U(0) = 0$ such that

$$\begin{aligned}(g, \hat{P}_H f) &= -i\hbar g^* f r^2|_0^\infty + \int_0^\infty r\mathrm{d}r\left[-i\hbar\left(r\frac{\partial}{\partial r} + 1\right)g\right]^* f \\ &= (\hat{P}_H g, f).\end{aligned} \tag{2}$$

This shows that the hyperbolic momentum operator is Hermitian. We further exploit the von Neumann method to explore the question concerning its self-adjoint nature [31]. Considering the eigenvalue equation $\hat{P}_H\psi = \pm i\gamma\psi$, where γ is a real and positive constant that has the dimension of $\hbar$, we find that both of the two solutions $\psi_\pm = C_\pm r^{\mp\gamma/\hbar - 1}$ cannot be normalized in its defined domain. Their respective dimensions of the normalized solution spaces, i.e., the deficiency indices, $n_- = 0$ and $n_+ = 0$, which proves that $\hat{P}_H$ is self-adjoint and can represent a physical observable. The hyperbolic momentum eigenstate can be derived from Eq. (1) as

$$\varphi_{P_H}(r) = \langle r|P_H\rangle = \frac{1}{\sqrt{2\pi\hbar}} r^{\frac{iP_H}{\hbar} - 1}, \tag{3}$$

where P_H is the eigenvalue that satisfies $\hat{P}_H\varphi_{P_H}(r) = P_H\varphi_{P_H}(r)$.

It is obvious that the radial position is defined in the domain $[0, \infty)$. Performing a coordinate transformation, we introduce the logarithmic radial position operator $\ln\hat{r}$, defined in the same domain. One can easily verify that the hyperbolic momentum and logarithmic radial position are a pair of conjugate variables, which satisfy the fundamental commutation relation $[\ln\hat{r}, \hat{P}_H] = i\hbar$, and consequently the relation between the uncertainties in logarithmic radial position, $\Delta \ln r$, and hyperbolic momentum, ΔP_H, has the form

$$\Delta \ln r \cdot \Delta P_H \geq \frac{\hbar}{2}, \tag{4}$$

which is bounded by Planck's constant. This means that for a state with a given uncertainty in its logarithmic radius, the hyperbolic momentum spectrum cannot be smaller than dictated by the radial uncertainty relation, and vice versa. Conversely, at the waist of a beam where the hyperbolic momentum is zero

(as the beam is neither converging nor dilating), the uncertainty in logarithmic radius must be infinite.

In the following we investigate the radial uncertainty relation by examining the limiting case of the intelligent states, i.e., those obeying the equality in Eq. (4). As the uncertainty product is bounded by a constant, these intelligent states coincide with the minimum uncertainty states. We can obtain the radial profile of the intelligent states $\Psi_i(r)$ by solving the equation

$$(\hat{P}_H - \langle \hat{P}_H \rangle)\Psi_i = i\hbar\lambda(\ln \hat{r} - \langle \ln \hat{r} \rangle)\Psi_i, \tag{5}$$

where $\langle \hat{P}_H \rangle$ and $\langle \ln \hat{r} \rangle$ denote the mean values of the hyperbolic momentum and its conjugate variable, the logarithmic radial position, respectively, and λ is a real constant [34]. We identify the normalized wave function of the intelligent states as

$$\Psi_i(r) = \frac{\lambda^{1/4} \exp\left[-\frac{\lambda}{2}(\ln r)^2 + \left(\lambda \overline{\ln r} - \frac{\overline{P_H}}{i\hbar} - 1\right)\ln r\right]}{\sqrt{\exp[\lambda(\overline{\ln r})^2]\pi^{1/2}}}, \tag{6}$$

where $\lambda = 1/[2(\Delta \ln r)^2]$ represents the variance of the logarithmic radial position, and $\overline{\ln r} = \langle \ln \hat{r} \rangle$ and $\overline{P_H} = \langle \hat{P}_H \rangle$ denote the average logarithmic radius and hyperbolic momentum, respectively. While linear position and momentum, and angular position and angular momentum are linked by Fourier transforms and series, the logarithmic radial position and hyperbolic momentum are linked by a quantum Mellin transform [30], allowing us to derive the hyperbolic momentum representation of the intelligent states as

$$\begin{aligned}\Psi_i(P_H) &= \int \Psi_i(r)\varphi^*_{P_H}(r)r\mathrm{d}r \\ &= \frac{\exp\left[(P_H - \overline{P_H})(-2i\hbar\lambda\overline{\ln r} - P_H + \overline{P_H})\right]}{2\hbar^2\lambda} \Big/ \sqrt{\hbar\sqrt{\lambda\pi}}.\end{aligned} \tag{7}$$

It is obvious that while the familiar Fourier transform decomposes the wave function in configuration space as a sum of plane waves defined in $(R, \mathrm{d}x)$, the decomposition of the quantum Mellin transform is defined in semi-definite space $(R^+, r\mathrm{d}r)$. These two representations are equivalent and connected by setting $x = \ln r$ and $\mathrm{d}x = \mathrm{d}r/r$, including a formal equivalence between the linear momentum and hyperbolic momentum. The profile of the intelligent states is proportional to $|\Psi_i|^2$, and the magnitude of the hyperbolic momentum spectrum can be obtained as $A_{P_H} = |\Psi_i(P_H)|^2$.

For the radial intelligent states, parameterized in λ, we find the uncertainty in logarithmic radial position to be $\Delta \ln r = \sqrt{\langle \Psi_i|(\ln \hat{r})^2|\Psi_i\rangle - (\langle \Psi_i|\ln \hat{r}|\Psi_i\rangle)^2} = \sqrt{1/2\lambda}$, and the uncertainty in hyperbolic momentum derived from Eq. (7) is $\Delta P_H = \hbar\lambda\Delta \ln r = \hbar\sqrt{\lambda/2}$. This allows us to confirm that the radial intelligent states satisfy the equality in the uncertainty relation as $\Delta \ln r \cdot \Delta P_H = \hbar/2$. In contrast, states with any other radial profile than the intelligent states will result in an uncertainty product exceeding the limit of $\hbar/2$.

3. EXPERIMENTAL IMPLEMENTATION

In the following we illustrate the radial uncertainty relation [Eq. (4)] by preparing light beams with radial profiles corresponding to various radial intelligent states as well as states with ring-shaped apertures. The experimental implementation is shown in Fig. 1. The incident beam is generated by a helium–neon laser with the center wavelength at 633 nm. We design various holograms to manipulate the radial positions with variable radial uncertainties $\Delta \ln r$ with fixed mean values of $\overline{\ln r} = \ln 1.6$ mm and $\overline{P_H} = 0$. A spatial light modulator (SLM) is used to display specific holograms that shape the desired radial positions, giving us flexible control over the transmitted light beam. After illumination with the incident plane wave, the first-order diffracted beam that has the amplitudes and phases of the intelligent states as expressed in Eq. (6) is filtered out. Then, a set of elaborate holographic gratings as described in Eq. (3) is prepared and displayed on another SLM, acting as projective measurements [see Fig. 1(b)]. For accurate measurements, it has been considered an absolute necessity that the intelligent states wave function and the hyperbolic momentum are centered with respect to the illuminating beam. A lens is used to Fourier transform the transmitted beam

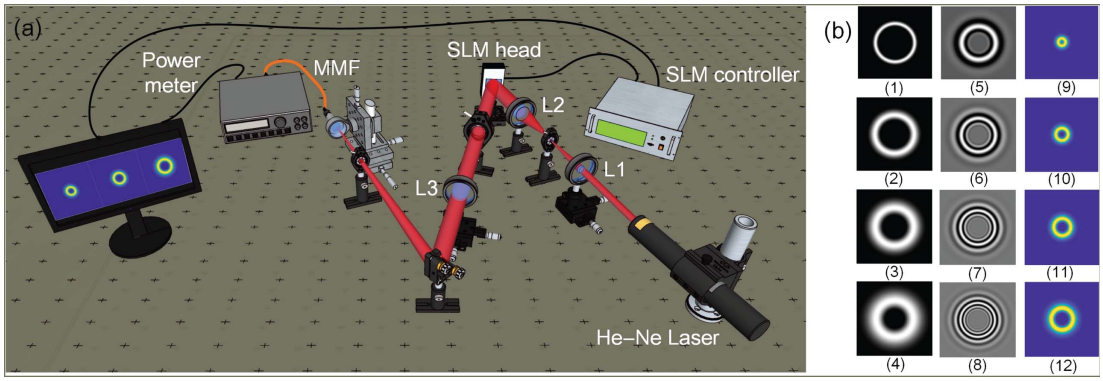

Fig. 1. (a) Experimental setup. The intelligent states with various uncertainties in logarithmic radial position such as (b1) $\lambda = 200.00$ ($\Delta \ln r = 0.05$), (b2) $\lambda = 50.00$ ($\Delta \ln r = 0.1$), (b3) $\lambda = 22.22$ ($\Delta \ln r = 0.15$), and (b4) $\lambda = 12.50$ ($\Delta \ln r = 0.2$) are displayed on the SLM. In addition, a set of well-elaborated holograms for analyzing the hyperbolic momentum is also displayed on the same SLM. A combination of these two holograms with fixed $\lambda = 12.50$ and (b5) $P_H = 10$, (b6) $P_H = 15$, (b7) $P_H = 20$, and (b8) $P_H = 25$ is shown in the middle column of (b). (b9–b12) show the resultant light beams in the Fourier plane.

such that the hyperbolic momentum spectrum is observed in the representation of the intelligent state. Finally, the light beam is coupled into a multimode fiber with a core size of 400 μm, and its intensity is measured by a power meter, providing the coefficients of the respective hyperbolic momentum component. The hologram for shaping the radial wave function of the input state corresponds to state preparation, and the hologram projecting onto a sequence of hyperbolic momentum states to state analysis. However, without loss of generality, a multiplexed hologram can instead be displayed on a single SLM. This is a common procedure to reduce the number of required optical components, ease alignment, and improve optical efficiency and hence signal-to-noise ratios.

To investigate the relation between logarithmic radial position and hyperbolic momentum, we prepare various intelligent states by setting $\lambda \in [8,200]$, yielding uncertainties of logarithmic radial position within the range of $\Delta \ln r \in [0.05,0.25]$, which can be displayed on our SLM with high accuracy. For maximal accuracy and signal-to-noise ratio of the measurement, we choose the core size of the multimode fiber, 400 μm, as the filtering diameter for the diffracted light beam. Figure 2 shows the experimental observation of the hyperbolic momentum spectrum, and the lower bound (red line) as obtained from theoretical prediction. Our measurement results agree well with the theoretical prediction, where slight deviations can be attributed to imperfect experimental components. Specifically, the experimental modulation of the small value of $\Delta \ln r$ in Fig. 2(a) is limited by the resolution and modulation accuracy of the SLM, resulting in a slight underestimate of ΔP_H. In contrast, the experimental modulation of the large value of $\Delta \ln r$ in Fig. 2(c) is affected by the detrimental noise arising from imperfections in filtering, correspondingly resulting in an overestimation of ΔP_H.

Figure 3 shows the experimentally observed product of the uncertainties in logarithmic radial position and hyperbolic momentum. We note that the experimental measurements are subject to the errors both in $\Delta \ln r$ and in ΔP_H. For small values of $\Delta \ln r$, the resolution and the modulation precision of the SLM significantly limit the experimental accuracy, resulting in an underestimation of ΔP_H. Conversely, for large values of $\Delta \ln r$, the noise from other values as a direct result of the imperfect filtering leads to an overestimation of ΔP_H, thus the product of $\Delta \ln r \cdot \Delta P_H$ becomes larger with respect to the increase of $\Delta \ln r$. The effects of filtering have been described in detail in Ref. [35]. In the ideal case, the product of the uncertainties in

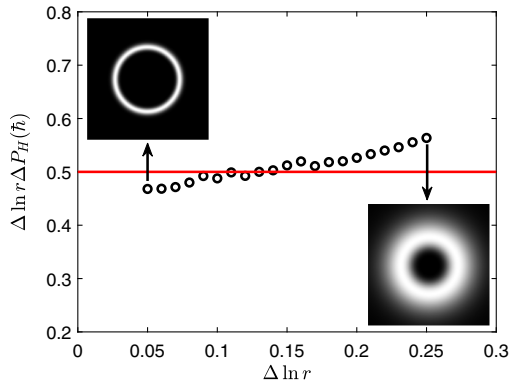

Fig. 3. Experimental measurement of the product of the uncertainties in logarithmic radial position and hyperbolic momentum for intelligent states. The red line represents the theoretical bound of $\hbar/2$.

logarithmic radial position and hyperbolic momentum equals $\hbar/2$ if the spatial filtering is extremely limited. However, the degree of spatial filtering determines the signal-to-noise ratio, and its increase would result in the detrimental errors. Therefore, a trade-off between signal-to-noise ratio and measurement accuracy of hyperbolic momentum is of great concern.

We note again that our intelligent states coincide with the minimum uncertainty-product state for the uncertainty

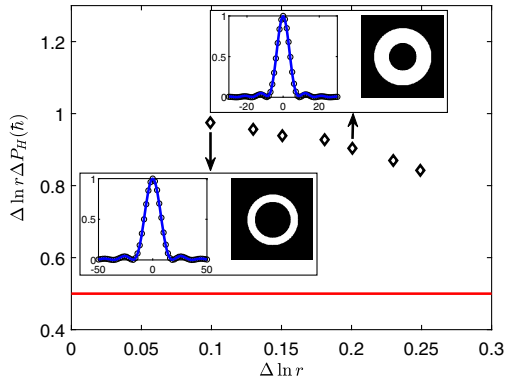

Fig. 4. Experimental measurement of the product of the uncertainties in logarithmic radial position and hyperbolic momentum for rigid slits. The red line represents the lower bound of $\hbar/2$ in the uncertainty relation (that can only be achieved by the intelligent states) as demonstrated in Eq. (4).

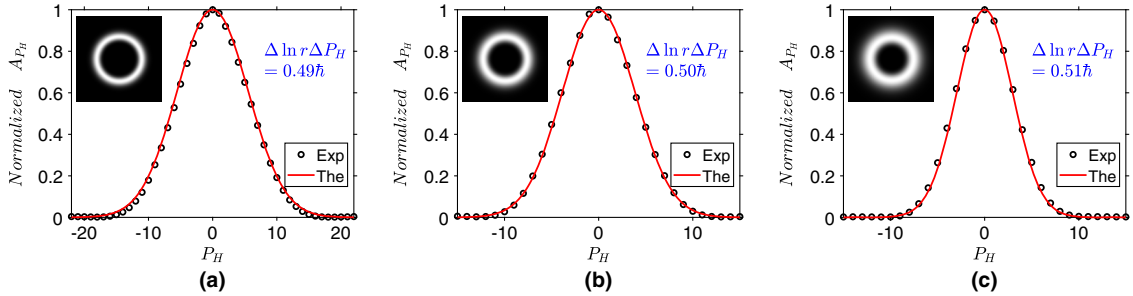

Fig. 2. Experimental observation of hyperbolic momentum spectrum for (a) $\lambda = 61.73$ ($\Delta \ln r = 0.09$), (b) $\lambda = 29.59$ ($\Delta \ln r = 0.13$), and (c) $\lambda = 17.30$ ($\Delta \ln r = 0.17$). The insets show the corresponding intelligent states displayed on the SLM.

relation of logarithmic radial position and hyperbolic momentum. This means that the uncertainty product for any other state is larger than this lower bound of $\hbar/2$. We further explore the uncertainty relation in experiments with rigid ring apertures, as shown in Fig. 4. While the product of the uncertainties for rigid ring apertures should be, in principle, infinite, experimental constraints necessarily "soften" the rigid edge, yielding finite value for the uncertainty product, but obviously larger than the lower bound.

4. DISCUSSION

In analogy to the uncertainty relation between linear and angular position and momentum, we have demonstrated the rigorous uncertainty principle for the radial degree of freedom. Unlike the analogous form of linear and angular variables, the canonical definition of the radial momentum has some subtle problems in history since the radial position is semi-definite. Even further, the canonical radial momentum is not self-adjoint such that it cannot present a physical observable. In this regard, our work suggests that the hyperbolic momentum operator has a self-adjoint extension, and thus it is a well-formed observable of radial momentum. Instead of radial position, we use logarithmic radial position to avoid the barrier of the semi-definite domain. Backed by these mathematical foundations, we presented a rigorous uncertainty principle for radial position and radial momentum, and derived radial intelligent states that provide the minimal radial uncertainty product. We have investigated the radial uncertainty experimentally, specifically confirming an uncertainty product of $\hbar/2$ for intelligent states over a wide range of radial uncertainties.

The radial uncertainty, just like linear and angular uncertainty relations, is a direct consequence of Fourier optics and holds in the classical regime, as demonstrated here. Nevertheless, it holds for individual photons within the classical light beam, and it would be interesting to perform a related experiment with a single photon source. Our results reveal that these two well-defined radial variables can provide a new platform for the fundamental tests of quantum mechanics, as well as for a variety of novel quantum information applications.

Funding. Program for New Century Excellent Talents in University of China (NCET-13-0495); Natural Science Foundation of Fujian Province of China for Distinguished Young Scientists (2015J06002); Fundamental Research Funds for the Central Universities at Xiamen University (20720190057); National Natural Science Foundation of China (12004318, 12034016, 61975169).

Disclosures. The authors declare no conflicts of interest.

Data Availability. Data underlying the results presented in this paper are not publicly available at this time but may be obtained from the authors upon reasonable request.

REFERENCES

1. W. Heisenberg, "Über den anschaulichen inhalt der quantentheoretischen kinematik und mechanik," Z. Phys. **43**, 172–198 (1927).
2. W. Heisenberg, *The Physical Principles of the Quantum Theory*, Dover Books on Physics and Chemistry (Dover, 1949).
3. H. P. Robertson, "The uncertainty principle," Phys. Rev. **34**, 163–164 (1929).
4. S. Franke-Arnold, S. M. Barnett, E. Yao, J. Leach, J. Courtial, and M. Padgett, "Uncertainty principle for angular position and angular momentum," New J. Phys. **6**, 103 (2004).
5. H. He, M. E. J. Friese, N. R. Heckenberg, and H. Rubinsztein-Dunlop, "Direct observation of transfer of angular momentum to absorptive particles from a laser beam with a phase singularity," Phys. Rev. Lett. **75**, 826–829 (1995).
6. A. Mair, A. Vaziri, G. Weihs, and A. Zeilinger, "Entanglement of the orbital angular momentum states of photons," Nature **412**, 313–316 (2001).
7. D. G. Grier, "A revolution in optical manipulation," Nature **424**, 810–816 (2003).
8. J. B. Götte, S. Franke-Arnold, and S. M. Barnett, "Angular EPR paradox," J. Mod. Opt. **53**, 627–645 (2006).
9. N. Bozinovic, Y. Yue, Y. Ren, M. Tur, P. Kristensen, H. Huang, A. E. Willner, and S. Ramachandran, "Terabit-scale orbital angular momentum mode division multiplexing in fibers," Science **340**, 1545–1548 (2013).
10. M. P. Lavery, F. C. Speirits, S. M. Barnett, and M. J. Padgett, "Detection of a spinning object using light's orbital angular momentum," Science **341**, 537–540 (2013).
11. V. D'ambrosio, N. Spagnolo, L. Del Re, S. Slussarenko, Y. Li, L. C. Kwek, L. Marrucci, S. P. Walborn, L. Aolita, and F. Sciarrino, "Photonic polarization gears for ultra-sensitive angular measurements," Nat. Commun. **4**, 2432 (2013).
12. F. Bouchard, J. Harris, H. Mand, R. W. Boyd, and E. Karimi, "Observation of subluminal twisted light in vacuum," Optica **3**, 351–354 (2016).
13. Á. S. Sanz and S. Miret-Artés, *A Trajectory Description of Quantum Processes. I. Fundamentals: A Bohmian Perspective* (Springer, 2012), Vol. **850**.
14. J. Oppenheim and S. Wehner, "The uncertainty principle determines the nonlocality of quantum mechanics," Science **330**, 1072–1074 (2010).
15. E. Karimi and E. Santamato, "Radial coherent and intelligent states of paraxial wave equation," Opt. Lett. **37**, 2484–2486 (2012).
16. E. Karimi, R. W. Boyd, P. de la Hoz, H. de Guise, J. R. Řeháček, Z. Hradil, A. Aiello, G. Leuchs, and L. L. Sánchez-Soto, "Radial quantum number of Laguerre-Gauss modes," Phys. Rev. A **89**, 063813 (2014).
17. W. N. Plick and M. Krenn, "Physical meaning of the radial index of Laguerre-Gauss beams," Phys. Rev. A **92**, 063841 (2015).
18. D. Geelen and W. Löffler, "Walsh modes and radial quantum correlations of spatially entangled photons," Opt. Lett. **38**, 4108–4111 (2013).
19. E. Karimi, D. Giovannini, E. Bolduc, N. Bent, F. M. Miatto, M. J. Padgett, and R. W. Boyd, "Exploring the quantum nature of the radial degree of freedom of a photon via Hong-Ou-Mandel interference," Phys. Rev. A **89**, 013829 (2014).
20. D. Zhang, X. Qiu, W. Zhang, and L. Chen, "Violation of a Bell inequality in two-dimensional state spaces for radial quantum number," Phys. Rev. A **98**, 042134 (2018).
21. P. D. Robinson and J. O. Hirschfelder, "Generalized momentum operators in quantum mechanics," J. Math. Phys. **4**, 338–347 (1963).
22. K. Fujikawa, "Non-Hermitian radial momentum operator and path integrals in polar coordinates," Prog. Theor. Phys. **120**, 181–195 (2008).
23. P. A. M. Dirac, *The Principles of Quantum Mechanics* (Oxford University, 1981), Vol. **27**.
24. L. Chen, T. Ma, X. Qiu, D. Zhang, W. Zhang, and R. W. Boyd, "Realization of the Einstein-Podolsky-Rosen paradox using radial position and radial momentum variables," Phys. Rev. Lett. **123**, 060403 (2019).
25. T. Ma, D. Zhang, X. Qiu, Y. Chen, and L. Chen, "Radial diffraction of light in the radial momentum state space," Opt. Lett. **45**, 5152–5155 (2020).

26. M. N. O'Sullivan-Hale, I. Ali Khan, R. W. Boyd, and J. C. Howell, "Pixel entanglement: experimental realization of optically entangled $d = 3$ and $d = 6$ qudits," Phys. Rev. Lett. **94**, 220501 (2005).
27. N. H. Valencia, V. Srivastav, M. Pivoluska, M. Huber, N. Friis, W. McCutcheon, and M. Malik, "High-dimensional pixel entanglement: efficient generation and certification," Quantum **4**, 376 (2020).
28. E. Ben-Eliezer, E. Marom, N. Konforti, and Z. Zalevsky, "Radial mask for imaging systems that exhibit high resolution and extended depths of field," Appl. Opt. **45**, 2001–2013 (2006).
29. J. Twamley, "Quantum distribution functions for radial observables," J. Phys. A **31**, 4811–4819 (1998).
30. J. Twamley and G. J. Milburn, "The quantum Mellin transform," New J. Phys. **8**, 328 (2006).
31. G. Bonneau, J. Faraut, and G. Valent, "Self-adjoint extensions of operators and the teaching of quantum mechanics," Am. J. Phys. **69**, 322–331 (2001).
32. V. S. Araujo, F. A. B. Coutinho, and J. F. Perez, "Operator domains and self-adjoint operators," Am. J. Phys. **72**, 203–213 (2004).
33. G. Paz, "The non-self-adjointness of the radial momentum operator in n dimensions," J. Phys. A **35**, 3727–3731 (2002).
34. E. Merzbacher, *Quantum Mechanics* (Wiley, 1961).
35. N. Radwell, R. F. Offer, A. Selyem, and S. Franke-Arnold, "Optimisation of arbitrary light beam generation with spatial light modulators," J. Opt. **19**, 095605 (2017).